Room temperature continuous wave lasing in InAs quantum-dot microdisks with air cladding

Toshihide Ide and Toshihiko Baba

Yokohama National University, Department of Electrical and Computer Engineering
79-5 Tokiwadai, Hodogaya-ku, Yokohama 240-8501, Japan
baba@ynu.ac.jp

Jun Tatebayashi, Satoshi Iwamoto, Toshihiro Nakaoka, and Yasuhiko Arakawa

University of Tokyo, Research Center for Advanced Science and Technology
4-6-1 Komaba, Meguro-ku, Tokyo 153-8904, Japan

Abstract: We demonstrated the first room temperature continuous wave lasing in InAs quantum-dot microdisk lasers with a standard air-cladding optical confinement structure. The spectrum shows the single strong lasing peak at a wavelength of 1280 nm. The threshold pump power is 410 μW, and the corresponding effective threshold obtained by considering the absorption efficiency is 81 μW. This achievement is mainly attributed to the increase in *Q* factor by the improved disk shape.

OCIS codes: (140.5960) Semiconductor lasers; (230.3990) Microstructure devices; (999. 9999) Quantum-dot

References and links

1. Y. Arakawa, and H. Sakaki, "Multidimensional quantum well laser and temperature dependence of its threshold current," Appl. Phys. Lett. **40,** 939-941 (1982).
2. M. Asada, Y. Miyamoto, and Y Suamatsu, "Gain and Threshold of Three-Dimensional Quantum-Box Lasers," IEEE J. of Quantum Electron. **QE-22,** 1915-1921 (1986).
3. S. L. McCall, A. F. J. Levi, R. E. Slusher, S. J. Pearton, and R. A. Logan, "Whispering-gallery mode microdisk lasers," Appl. Phys. Lett. **60,** 289-291 (1992).
4. M. Fujita, R. Ushigome, and T. Baba, "Continuous wave lasing in GaInAsP microdisk injection laser with threshold current of 40 μA," Electorn. Lett. **36,** 169-170 (2000).
5. T. Baba, and D. Sano, "Low-threshold lasing and Purcell effect in microdisk lasers at room temperature," IEEE J. Sel. Top. Quantum Electron. **9,** 1340-1346 (2003).
6. B. Gayral, J. M. Gerard, A. Lemaitre, C. Dupuis, L. Manin, and J. L. Pelouard, "High-*Q* wet-etched GaAs microdisks containing InAs quantum boxes," Appl. Phys. Lett. **75,** 1908-1910 (1999).
7. H. Cao, J. Y. Xu, W. H. Xiang, Y. Ma, S.-H. Chang, S. T. Ho, and G. S. Solomon, "Optically pumped InAs quantum dot microdisk lasers," Appl. Phys. Lett. **76,** 3519-3521 (2000).
8. P. Michler, A. Kiraz, L. Zhang, C. Becher, E. Hu, and A. Imamoglu, "Laser emission from quantum dots in microdisk structures," Appl. Phys. Lett. **77,** 184-186 (2000).
9. K. J. Luo, J. Y. Xu, H. Cao, Y. Ma, S. H. Chang, S. T. Ho, and G. S. Solomon, "Ultrafast dynamics of InAs/GaAs quantum-dot microdisk lasers," Appl. Phys. Lett. **78,** 3397-3399 (2001).
10. L. Zhang, and E. Hu, "Lasing from InGaAs quantum dots in an injection microdisk," Appl. Phys. Lett. **82,** 319-321 (2003).
11. T. Yang, J. Cao, P. Lee, M. Shih, R. Shafiiha, S. Farrell, J. O'Brien, O. Shchekin, and D. Deppe, "Microdisks with quantum dot active regions lasing near 1300 nm at room temperature," *in Tech. Dig. Conf. on Lasers and Electro-Optics*, (The Optical Society of America, Washington, DC, 2003), CWK3.
12. T. Ide, T. Baba, J. Tatebayashi, S. Iwamoto, T. Nakaoka, and Y. Arakawa, "Lasing characteristics of InAs quantum-dot microdisk from 3K to room temperature," Appl. Phys. Lett. **85,** 1326-1328 (2004).
13. T. Yang, O. Shchekin, J. D. O'Brien, and D. G. Deppe, "Room temperature, continuous-wave lasing near 1300 nm in microdisks with quantum dot active regions," Electron. Lett. **39,** 1657-1658 (2003).
14. J. Tatebayashi, M. Nishioka, and Y. Arakawa, "Over 1.5 μm light emission from InAs quantum dots embedded

#6241 - $15.00 US Received 6 January 2005; revised 23 February 2005; accepted 23 February 2005

in InGaAs strain-reducing layer grown by metalorganic chemical vapor deposition," Appl. Phys. Lett. **78,** 3469-3471 (2001).
15. K. Nozaki, A. Nakagawa, D. Sano, and T. Baba, "Ultralow threshold and single-mode lasing in microgear lasers and its fusion with quasi-periodic photonic crystals," IEEE J. Sel. Top. Quantum Electron. **9**, 1355-1360 (2003).
16. R. Heits, I. Mukhametzhanov, A. Madhukar, A. Hoffmann, and D. Bimberg, "Temperature dependent optical properties of self-organized InAs/GaAs quantum dots," J. Electron. Mater. **28**, 520-527 (1999)
17. M. Fijita, K. Teshima, and T. Baba, "Low-threshold continuous-wave lasing in photopumped GaInAsP microdisk lasers," Jpn. J. Appl. Phys. **40**, L875-L877 (2001).
18. J. L. Jewell, J. P. Harbison, A. Scherer, Y. H. Lee, and L. T. Florez "Vertical-cavity surface-emitting lasers: design, growth, fabrication, characterization," IEEE J. Quantum Electron. **27,** 1332-1346 (1991).
19. R. Ushigome, M. Fujita, A. Sakai, T. Baba, and Y. Kokubun, "GaInAsP microdisk injection laser with benzocyclobutene polymer cladding and its athermal effect," Jpn. J. Appl. Phys. **41,** 6364-6369 (2002).

The quantum-dot (QD) active region in semiconductor lasers is effective for low threshold, high-speed and temperature-insensitive lasing, and for turnstile operation due to the strong electronic confinement [1,2]. On the other hand, the microdisk laser (MDL) is effective for low threshold lasing and high-speed spontaneous emission due to the strong optical confinement [3,4]. When the QD active region is used for the MDL, not only their combined effects but also suppression of the surface recombination at the disk sidewall are expected because the carrier diffusion is suppressed by QDs. Thus, the QD MDL is a promising candidate for ultralow threshold integrated laser sources and high-speed and high-efficiency single-photon emitters [5]. However, most reports on this device have only described the low temperature operation [6-10]. The main reason for this is an insufficient number of QDs and the corresponding low optical gain. Recently, Yang, et al. and our group employed the five-stacked InAs QD layers and achieved the room temperature (RT) lasing by pulsed photopumping [11,12]. However, the RT continuous wave (cw) lasing was reported only for a cylinder-type laser with the oxidized AlAs cladding [13]. The thermal resistance of the cylinder type is lower than that of the standard MDL with the air cladding. Therefore, the RT cw lasing may be obtained more easily. However, the optical confinement of the cylinder type is much weaker than that of the standard MDL, which is out of interest in this study. Previously, we investigated pulsed lasing characteristics of the InAs QD MDL from 3 K to RT and observed the rapid increase in threshold and decrease in slope efficiency above 200 K [12]. At RT, the effective threshold power obtained by considering the pump efficiency was 750 μW and the corresponding threshold density was 4.7 kW/cm^2. These values are one order of magnitude higher than those of GaInAsP compressively strained quantum-well (CSQW) MDLs. It indicates that the threshold reduction by the increase in *Q* factor is necessary for the RT cw lasing in QD MDLs. In this study, we improved the disk shape by optimizing the dry etching process, and achieved the RT cw lasing of this device.

In the experiment, GaAs buffer, $Al_{0.6}Ga_{0.4}As$ clad, QD active region, $Al_{0.6}Ga_{0.4}As$ clad and GaAs cap layer were successively grown on GaAs substrate by metal organic vapor phase epitaxy. Five-stacked InAs QD layers were grown by Stranski-Krastanow mode with InGaAs buried layers. The density of the QDs was 2.0×10^{10} cm^{-2}. Details of the active region and growth condition are described in other reports [12,14]. In the fabrication process, a circular mesa was formed by *e*-beam lithography and Cl_2/Xe inductively coupled plasma etching. By controlling the etch rate of GaAs to be higher than that of $Al_{0.6}Ga_{0.4}As$, the symmetric and concave mesa sidewall was formed. On this condition, the active region was slightly side-etched, so the vertical sidewall of the active region was formed. Finally, the disk shape and the pedestal were formed by HF at RT for ~10 s. Figure 1 shows a 4.5-μm-diameter device. The angle of the disk sidewall is 80°, which is improved from 50° of the previous device [12]. In the measurement, the MDL was photopumped by cw light of Ti-sapphire laser at wavelength λ = 780 nm with a focused spot diameter of ~2 μm. Light output was analyzed

#6241 - $15.00 US Received 6 January 2005; revised 23 February 2005; accepted 23 February 2005

by a monochrometer with InGaAs charge-coupled device array.

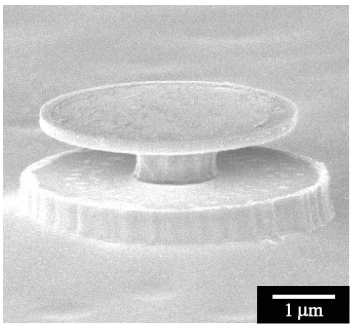

Fig. 1. Scanning electron microscope image of 4.5-μm-diameter QD MDL.

Figure 2 shows the intensity of a mode peak at λ = 1280 nm at RT. The lower horizontal axis is the irradiated power P_{irr} of the pump light to the MDL. By considering the multiple absorption in the disk expressed as $(1 - R)[1 - \exp(-\alpha d)]/[1 - R \exp(-\alpha d)]$ with a disk thickness d = 0.185 μm, reflectivity at the disk surface R ~ 30% and average absorption coefficient inside the disk $\alpha \sim 13000$ cm^{-1}, P_{irr} is converted to the effective pump power P_{eff}, as shown on the upper horizontal axis of Fig. 2 [15]. The intensity exhibits a clear kink at threshold. The irradiated threshold power is 410 μW, and the corresponding effective threshold is 81 μW. These values are much lower than an irradiated threshold power of 2 mW and an effective threshold of 0.2 mW reported for the cylinder-type laser [13]. The inset of Fig. 2 shows the lasing spectrum at P_{eff} = 170 μW. The RT photoluminescence (PL) spectrum of the QD wafer is also shown by the dotted line as a reference. Although ground state and first excited state energy levels of the QD wafer were designed to 1340 and 1270 nm, respectively, this spectrum shows the broad single peak due to large inhomogeneous broadening in the multi-stacked QD layers. The lasing spectrum shows the strong single peak at λ = 1280 nm. The maximum mode peak intensity is 20 dB higher than the background spontaneous emission level.

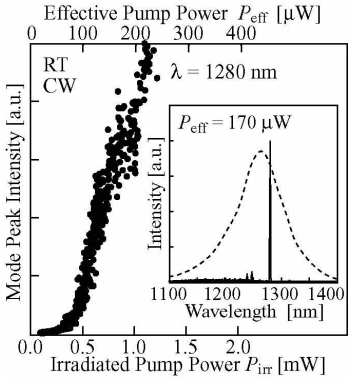

Fig. 2. RT lasing characteristic at λ = 1280 nm. Inset shows lasing spectrum at P_{eff} = 170 μW. Dotted-line is RT photoluminescence spectrum of the QD wafer.

Figure 3 shows lasing spectra with a wavelength resolution of 0.1 nm. As the pump power increases, the spectral narrowing is observed below threshold. The spectral full-width at half

#6241 - $15.00 US Received 6 January 2005; revised 23 February 2005; accepted 23 February 2005

maximum (FWHM) below threshold is 0.18 nm, and it reaches to 0.14 nm above threshold. This value is still larger than the resolution limit of the measurement system. It might be caused by the thermal redshift during the accumulation time of the spectral measurement. The *Q* factor is evaluated from the FWHM at 0.5 times the threshold to be 7100. This value is twice higher than the previous one [12]. We think that this *Q* factor is also slightly under-estimated due to the thermal redshift. Figure 4 shows the lasing wavelength shift with the effective pump power. The wavelength is redshifted by heating under cw operation. The thermal resistance R_t is estimated by the formula $R_t = dT/dW = (d\lambda/dT)^{-1} \cdot d\lambda/dW$. Here, $d\lambda/dT$ is the temperature dependence of the wavelength under pulse operation, which was separately evaluated to be 0.05 nm/K. On the other hand, $d\lambda/dW$ is estimated from the redshift in Fig. 4 to be 1.5 nm/mW. Thus, R_t is evaluated to be 3×10^4 K/W.

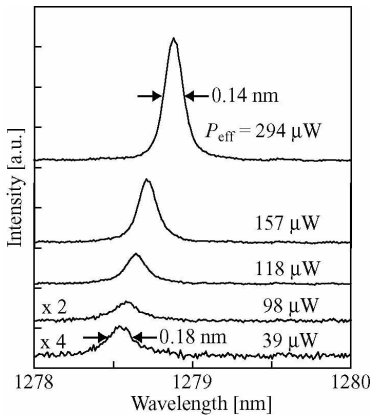

Fig. 3. Lasing spectra measured with a resolution of 0.1 nm.

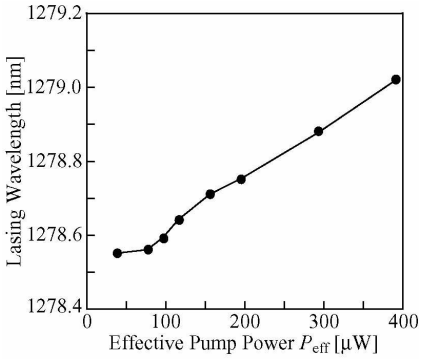

Fig. 4. Lasing wavelength with effective pump power.

Figure 5 shows the temperature dependence of the effective threshold and slope efficiency from 3 K to RT. The effective threshold below 130 K is less than 20 μW. Characteristic temperatures are 64 and 36 K in the temperature range of 130 – 230 K and above 230 K, respectively. The threshold rapidly increases in the range of 50 – 100 K as shown in the previous study [12]. It is considered to be due to the particular increase in carrier overflow by the long carrier diffusion length in this temperature range. The threshold above 230 K exceeds the value observed at RT before measuring the temperature dependence, and the lasing peak intensity became to be weak gradually due to the thermal degradation. The slope efficiency

#6241 - $15.00 US Received 6 January 2005; revised 23 February 2005; accepted 23 February 2005

decreases rapidly above 250 K due to free carrier absorption. Even with the thermal degradation, this temperature is improved from a previous value of 230 K [12]. It must be the effect of the low threshold. Figure 6 shows the temperature dependence of the lasing wavelength. The wavelength redshifts from 1210 to 1280 nm in the temperature range from 130 K to RT with showing the hopping of the whispering gallery mode of the MDL. The dotted line in Fig. 6 shows the theoretical bandgap shift ΔE_g of the QDs, which is estimated by Varshni's formula $\Delta E_g = AT^2/(T + B)$ (A and B are characteristic parameters for the semiconductor) [16]. The experimental redshift above 130 K is well explained by the theory with $A = 4.5 \times 10^{-4}$ eV/K and $B = 180$ K, which are typical value between InAs and GaAs bulk materials. In the previous study, we observed the saturation of the redshift above 250 K due to the carrier plasma effect by the high threshold carrier density. However, such saturation is not observed in Fig. 6, which suggests a low threshold carrier density.

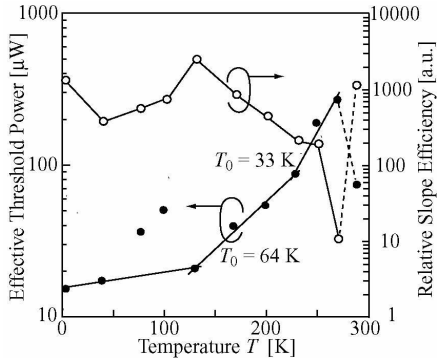

Fig. 5. Temperature dependence of effective threshold power (black) and slope efficiency (white). The data at RT (290 K) is obtained before measuring the temperature dependence.

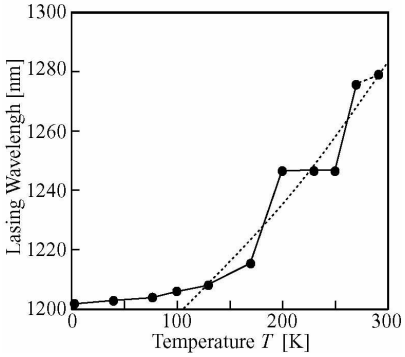

Fig. 6. Temperature dependence of lasing wavelength. Dotted line is theoretical calculation.

All of these results clearly indicate that the threshold was greatly reduced and overall lasing characteristics were improved. We compared the RT cw lasing characteristics of the QD MDL with those of conventional GaInAsP CSQW MDLs. Considering the disk diameter of 4.5 μm, the effective threshold power density of the QD MDL is estimated to be 510 W/cm^2. This value is almost comparable to 460 W/cm^2 of CSQW MDLs [5]. Since the optical confinement factor of the QD MDL (1.2%) is six times lower than that of CSQW MDLs (7 – 8%), the low threshold of the QD MDL should be attributed to other merits such as a high Q factor. The Q factor measured for the 3-μm-diameter CSQW MDL is 3000 [17]. Although the

#6241 - $15.00 US Received 6 January 2005; revised 23 February 2005; accepted 23 February 2005

diameter of the QD MDL in this study is slightly larger, the *Q* factor of the QD MDL is twice higher. However, the *Q* factor cannot still compensate for the low optical confinement factor. It suggests that a high material gain and low surface recombination by the QDs significantly contributed to the low threshold. The surface recombination of GaAs-based materials is $1 - 2$ orders higher than that of InP -based materials. Due to this effect, very limited number of GaAs-based microcavities have achieved the RT lasing [18]. Therefore, the low threshold of the QD MDL in this study cannot be expected, unless the surface recombination is greatly reduced by the low carrier diffusion in the QD active layer. The thermal resistance of the QD MDL is much lower than $\sim 1 \times 10^5$ K/W of the CSQW MDL with the same diameter [19]. A reason considered for this is that the QD MDL mainly consists of binary or semi-binary compound materials. We can say that the total characteristics of the QD MDL are almost comparable to those of CSQW MDLs. By decreasing the disk diameter and improving the uniformity of QDs, the threshold of the QD MDL will be lower than that of QW MDLs.

In conclusion, the RT cw lasing was achieved in the InAs QD MDL with the standard air-cladding structure by photopumping. The lasing wavelength was 1280 nm, and the effective threshold power was 81 μW. The main improvement was the increase in *Q* factor by the vertical sidewall of the disk. The temperature dependence from 3 K to RT showed various improvements arising from the threshold reduction. The total performance of the QD MDL is almost comparable to CSQW MDLs. We expect the near future that a smaller disk and higher *Q* factor achieve an ultimate low threshold and allow the electrical pumping operation.

Acknowledgments

This work was supported by The IT Program and The 21st Century COE Program from MEXT, The Grant-In-Aid from JSPS, and CREST Project from JST.

#6241 - $15.00 US Received 6 January 2005; revised 23 February 2005; accepted 23 February 2005